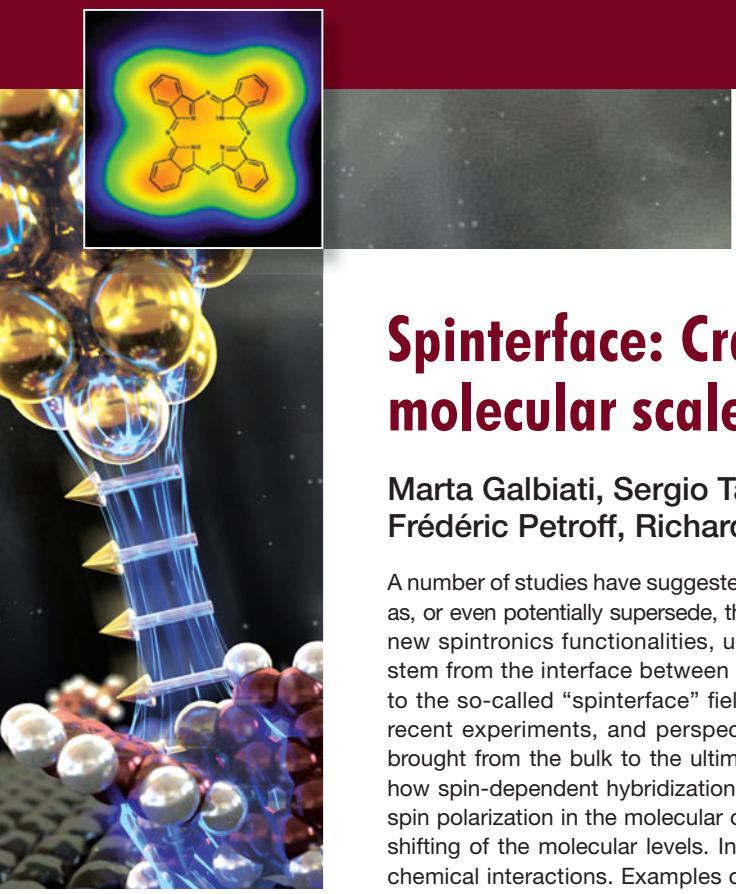

Spinterface: Crafting spintronics at the molecular scale

Marta Galbiati, Sergio Tatay, Clément Barraud, Alek V. Dediu, Frédéric Petroff, Richard Mattana, and Pierre Seneor

A number of studies have suggested that molecular materials could offer similar performance as, or even potentially supersede, those of inorganic materials in spintronics devices. Radically new spintronics functionalities, unavailable with conventional inorganic materials, could stem from the interface between ferromagnetic (FM) and molecular materials, giving rise to the so-called "spinterface" field. In this article, we review the fundamental concepts, recent experiments, and perspectives in this fast rising field, where the functionality is brought from the bulk to the ultimate downscaled device: the interface. The article shows how spin-dependent hybridization at the FM metal/molecule interface can lead to induced spin polarization in the molecular orbitals thanks to spin-dependent broadening and energy shifting of the molecular levels. Interfacial spin polarization can then be tailored thanks to chemical interactions. Examples of enhancement and reversal are given, and we highlight how this spin-dependent hybridization opens a new door for the spintronics crafting of multifunctionality through chemical designing and tuning on the molecular scale.

Introduction

In electronics and spintronics, interfaces between dissimilar materials are probably the most complex and difficult issues to handle. They are often viewed as a potential source of problems, especially in devices made of molecular materials. After a decade of breakthrough works highlighting the potential of organics,[1–5] only very recently has it been proposed that spin-dependent hybridizations at interfaces between ferromagnetic (FM) electrodes and molecular materials could pave the way to chemically designed, radically new multifunctional device concepts.[6] This led to the suggestion that tailoring spintronic devices may be achieved by exploiting such interface hybridization, which gave rise to a field now coined "spinterface science."[7] What was once thought to be an issue now becomes a key asset for tailoring spintronics properties to the point that tailoring at the nanoscale appears to be one of the most promising quests in spintronics.

In this article, we present spinterface science, a very recent but fast-rising field for which we review conceptual work, recent pioneering experiments, and give perspectives for spintronics manipulation. We first present how spin-hybridized states can drastically influence the spin transport properties of molecular spintronics devices and provide new functionalities beyond that of conventional inorganic ones. We also highlight how these spin-hybridized states contribute to define an "effective electrode." We finally give simple examples showing how spin-polarized hybridization at the interface can lead to a complete reversal of sign or to an enhancement of the effective electrode spin polarization.

Tailoring spintronics through molecular spin hybridization

We first start with what happens when the usual band structure of a solid-state device (**Figure 1**a) is replaced with discrete molecular states. Starting from this point, we first consider a discrete and isolated molecular level as in Figure 1b. Being isolated, the lifetime of this state is infinite, and its energy is precisely known (the time-energy equivalent to the Heisenberg uncertainty principle). But, what happens to this at an interface in a device? When brought in proximity to a

Marta Galbiati, Unité Mixte de Physique CNRS/Thales and Université Paris-Sud, France; marta.galbiati@thalesgroup.com
Sergio Tatay, Chemistry Institute for Molecular Science, University of Valencia, Spain; sergio.tatay@uv.es
Clément Barraud, Laboratoire Matériaux et Phénomènes Quantiques, Université Paris-Diderot, France; clement.barraud@univ-paris-diderot.fr
Alek V. Dediu, Institute of Nanostructured Materials, CNR-ISMN, Italy; v.dediu@bo.ismn.cnr.it
Frédéric Petroff, Unité Mixte de Physique CNRS/Thales and Université Paris-Sud, France; frederic.petroff@thalesgroup.com
Richard Mattana, Unité Mixte de Physique CNRS/Thales and Université Paris-Sud, France; richard.mattana@thalesgroup.com
Pierre Seneor, Unité Mixte de Physique CNRS/Thales and Université Paris-Sud, France; pierre.seneor@thalesgroup.com
DOI: 10.1557/mrs.2014.131

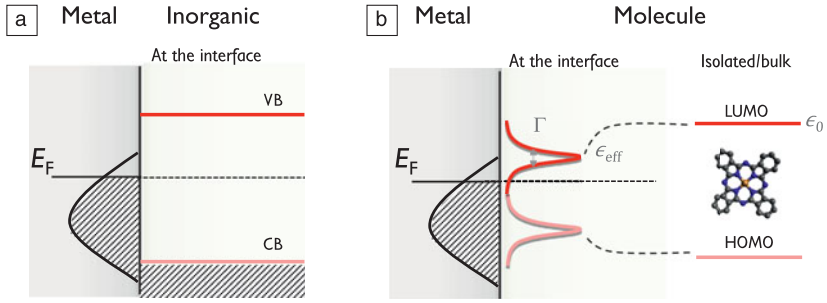

Figure 1. Schematic representation of (a) the interface between a metal and an inorganic material, such as a semiconductor or insulator, versus (b) what happens when an isolated molecule is brought in proximity with a metallic surface. For simplicity, a flat band configuration is used for the semiconductor in the first few nanometers from the interface. As opposed to the inorganic materials, molecules present discrete levels. When interacting with the metal, the initial discrete levels of the isolated molecule broaden and shift relative to the density of states of the metal. Note: E_F, metal Fermi energy level; CB, conduction band; VB, valence band; HOMO, highest occupied molecular orbital; LUMO, lowest unoccupied molecular orbital; Γ, molecular energy level broadening; ϵ_0 isolated molecular level energy; ϵ_{eff}, effective molecular level energy when coupled to the surface.

metallic electrode, the initially isolated molecular level gets progressively hybridized by coupling with the many states of the metal. The two main consequences are*:

(1) The lifetime (τ) on the molecular level is now finite, as there is a certain probability to escape to the metal. This, in turn, leads to a level energy broadening (i.e., the energy level is no more precisely known, similar to the uncertainty principle) with a finite width $\Gamma \approx \hbar / \tau$ (where $\hbar$ is the reduced Planck constant), which, in the first approximation, is proportional to the density of states (DOS) of the metal. Depending on the strength of the interaction, the broadening can range from below the meV regime for weak coupling up to the eV range for stronger interactions.[9]

(2) As a result of its interaction with the metal, the molecular energy level shifts from the isolated (gas-phase) value with energy ϵ_0, to an energy ϵ_{eff}, as shown in Figure 1b. This shift is dependent on the metal DOS and includes, among other contributions, the combined effect of interfacial dipoles or image forces.[10]

Spin-dependent hybridization

Barraud et al.[6] predicted that for a FM electrode, one could expect the energy shifting and broadening of the level to become spin-dependent. In FM metals, the DOS of the two spin directions are different $D^{\uparrow}_{FM}(E) \neq D^{\downarrow}_{FM}(E)$ (where $D^{\uparrow(\downarrow)}_{FM}(E)$ = DOS for a spin up (down) FM metal at energy E). Hence, the initially spin-degenerated molecular level would split with two different energies $\epsilon^{\uparrow}_{eff} \neq \epsilon^{\downarrow}_{eff}$ and two different broadening widths $\Gamma^{\uparrow} \neq \Gamma^{\downarrow}$ for the two spin directions, $\uparrow$ or $\downarrow$ (see **Figure 2**), respectively. The broadening and shifting are weighted by the individual coupling of each metallic state to the molecular state, and hence related to the metal DOS. For example, the spin-dependent broadening can be expressed as $\Gamma^{\uparrow(\downarrow)}(E) = 2\pi \sum_{i^{\uparrow(\downarrow)}} \left| V_{i^{\uparrow(\downarrow)}} \right|^2 \delta(E_i - E)$, where $V_{i^{\uparrow(\downarrow)}}$ is the coupling between the spin-dependent state $i^{\uparrow(\downarrow)}$ of the metallic electrode and the discrete molecular state, and $\sum_{i^{\uparrow(\downarrow)}} \delta(E_i - E)$ is the sum over all these states. Intuitively, one can obtain a simple picture and see that for a constant coupling, $V_{i^{\uparrow(\downarrow)}} \approx V$, the broadening is now directly proportional to the FM electrode DOS with $\Gamma^{\uparrow(\downarrow)}(E) \propto D^{\uparrow(\downarrow)}_{FM}(E)$. In a more realistic picture, for example, for a 3*d* ferromagnet (such as Co, Fe, and Ni), one would expect different contributions for *s* or *d* bands or even of different wave-function symmetries co-existing in the metal, as in crystalline MgO-based tunnel junctions.

The spin-dependent energy broadening and shifting created by the spin hybridization with the electrode will induce spin polarization of the molecular orbitals. This hybridization will strongly depend on the coupling strength between the FM metal and the molecule.

Defining a new electrode

It was proposed[6] that a new effective electrode could be defined by considering the original FM electrode together with the first spin hybridized molecular layer at the interface. The new effective electrode would be driven by the interface, and its DOS $D^{\uparrow(\downarrow)}_{Int}(E)$ could then be characterized by two key parameters, $\Gamma^{\uparrow(\downarrow)}$ and $\epsilon^{\uparrow(\downarrow)}_{eff}$, derived previously and from which one could simply predict the spintronics response of a device. Indeed, the effect of this spin-dependent broadening and shifting of the molecular level can be simply described through a Lorentzian distribution for its DOS:

$$D^{\uparrow(\downarrow)}_{Int}(E) = \frac{\Gamma^{\uparrow(\downarrow)}/2\pi}{\left(E - \epsilon^{\uparrow(\downarrow)}_{eff}\right)^2 + (\Gamma^{\uparrow(\downarrow)}/2)^2}. \quad (1)$$

This DOS is the effective electrode's (spinterface's) DOS, and it accounts for the original electrode contribution through $\Gamma^{\uparrow(\downarrow)}$ and $\epsilon^{\uparrow(\downarrow)}_{eff}$.† It can then be used to define the spin polarization of the spinterface:

* This overall contribution is usually accounted for by the concept of self-energy Σ, which takes into account the energy broadening $\Gamma = -2\ \mathrm{Im}(\Sigma)$ as well as the energy shift $\mathrm{Re}(\Sigma) = \epsilon_{eff} - \epsilon_0$ experienced by the level. One can refer to books, such as the one by Datta,[8] for more insight on this and the related concept of self-energy.

† Those parameters, characteristic of each spinterface, could be computed or extracted phenomenologically from transport measurements in solid-state devices or spectroscopic studies.

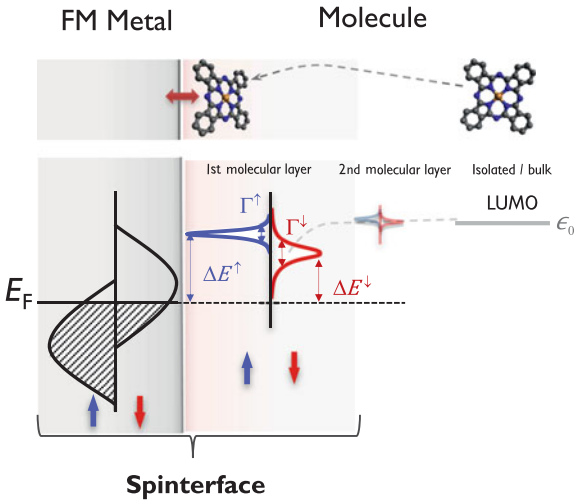

Figure 2. Schematic representation of the molecular hybridization at an interface with a ferromagnetic (FM) metal. (Top) Representation of the molecule as it gets closer to the surface and is progressively coupled with the FM metal. (Bottom) Representation of the metal density of states (DOS) and molecular orbitals for the corresponding position of the molecule. Molecules present discrete levels (far right) that shift and broaden as the hybridization with the metal grows stronger toward chemi/physi-sorption. As the spin up and spin down DOS are different in the FM metal, the broadening Γ and energy shifting Δ*E* become spin dependent on the molecule. This induces a spin polarization on the first molecular layer. A new effective electrode can be defined, including the first molecular layer, the spinterface. For simplicity, only the lowest unoccupied molecular orbit (LUMO) is represented for the molecule (the effect is also expected for the other orbitals); the 3*d* ferromagnet is represented with a simple band structure, whereas the *s* and *d* bands and anisotropy should be taken into account in the spin-dependent hybridization. Adapted from Reference 6. Note: E_F, metal Fermi energy level; difference between molecular level energy and metal Fermi level $\Delta E^{\uparrow(\downarrow)} = E_F - \epsilon_{eff}^{\uparrow(\downarrow)}$ with $\epsilon_{eff}^{\uparrow(\downarrow)}$ the effective molecular level energy for spin up (down); $\Gamma^{\uparrow(\downarrow)}$, energy level broadening for spin up (down).

$$P_{int} = \frac{D_{Int}^{\uparrow} - D_{Int}^{\downarrow}}{D_{Int}^{\uparrow} + D_{Int}^{\downarrow}}. \qquad (2)$$

To illustrate the tailoring opportunities arising from the spin-dependent hybridization and highlight the difference with the inorganic case, we focus on two examples,[6] illustrated in **Figure 3** that, may be ascribed to strong and weak molecule/metal interactions. We give limits for $D_{Int}^{\uparrow(\downarrow)}(E)$, where the broadening is much larger (smaller) than the level distance to the Fermi energy level, $\Gamma \gg \Delta E$ ($\Gamma \ll \Delta E$), with $\Delta E = E_F - \epsilon_{eff}^{\uparrow(\downarrow)}$ and E_F is the Fermi energy level.

The first example (shown in Figure 3b) corresponds to the case where $\Gamma \gg \Delta E$. From Equation 1, we obtain $D_{Int}^{\uparrow(\downarrow)} \approx \frac{1}{\Gamma^{\uparrow(\downarrow)}}$ and hence $D_{Int}^{\uparrow(\downarrow)} \propto \frac{1}{D_{FM}^{\uparrow(\downarrow)}}$. As a result, the effective spinterface DOS is now inversely proportional to the electrode's original DOS, and the sign of spin polarization at the interface (P_{int}) is the opposite of that for the original FM electrode (P_{FM}). From Equation 2:

$$P_{int} = -\frac{\Gamma^{\uparrow} - \Gamma^{\downarrow}}{\Gamma^{\uparrow} + \Gamma^{\downarrow}} \approx -\frac{D_{FM}^{\uparrow} - D_{FM}^{\downarrow}}{D_{FM}^{\uparrow} + D_{FM}^{\downarrow}} = -P_{FM}, \qquad (3)$$

one can get a physical picture by recalling that as the area of the broadening is constant (single initial spin state), a larger broadening ($\Gamma \propto D_{FM}^{\uparrow(\downarrow)}$) corresponds to a reduced maximum for the molecular DOS $D_{Int}^{\uparrow(\downarrow)}$. This explains the DOS inversion between the FM and the molecular state (see Figure 3b). This situation is initially expected to happen for intermediate to strong coupling, where Γ is expected to be large.[9] However, it could also happen for weaker Γ in a situation where $\epsilon_{eff}^{\uparrow(\downarrow)} \to E_F$ (i.e., $\Delta E \to 0$) due to the cumulative effect of image forces and dipoles.[10]

The second case, shown in Figure 3c, corresponds to the case where the molecular level is only slightly shifted, and the broadening Γ is small enough to be neglected with respect to Δ*E*. In this $\Gamma \ll \Delta E$ limit, from Equation 1 we obtain $D_{Int}^{\uparrow(\downarrow)} = \frac{\Gamma^{\uparrow(\downarrow)}}{\left(\Delta E^{\uparrow(\downarrow)}\right)^2}$ and hence $D_{Int}^{\uparrow(\downarrow)} \propto \frac{D_{FM}^{\uparrow(\downarrow)}}{\left(\Delta E^{\uparrow(\downarrow)}\right)^2}$. The effective spinterface DOS in this case is proportional to the electrode's original one (same spin polarization sign) but becomes levered by $\left(\Delta E^{\uparrow(\downarrow)}\right)^2$. The spin-dependent shift $\epsilon_{eff}^{\uparrow(\downarrow)}$ (found in $\left(\Delta E^{\uparrow(\downarrow)}\right)^2$) acts as a spin-filter effect.[‡11,12] As shown in Figure 3c, when the less (more) broadened level stays further away from (is brought closer to) the FM Fermi level, one can obtain an enhancement effect for the spin polarization, from Equation 2:

$$P_{int} = \frac{\frac{\Gamma^{\uparrow}}{\Delta E^{\uparrow 2}} - \frac{\Gamma^{\downarrow}}{\Delta E^{\downarrow 2}}}{\frac{\Gamma^{\uparrow}}{\Delta E^{\uparrow 2}} + \frac{\Gamma^{\downarrow}}{\Delta E^{\downarrow 2}}} > P_{FM}. \qquad (4)$$

This is more likely to be the most common case for weak coupling where the broadening is small with respect to $\Delta E = E_F - \epsilon_{eff}^{\uparrow(\downarrow)}$.

From this simple model, spin response can be strongly modulated by the hybridization at the interface. These results demonstrate considerable potential for spin polarization tailoring. Next, we focus on recent experimental evidence demonstrating the two functionalities described previously, highlighting the potential of the spinterface for spintronics.

‡ In a spin filter, a spin-polarized current is created by a spin-dependent shifting of the band structure of the tunnel barrier. For more information, see the review by Moodera et al.[11]

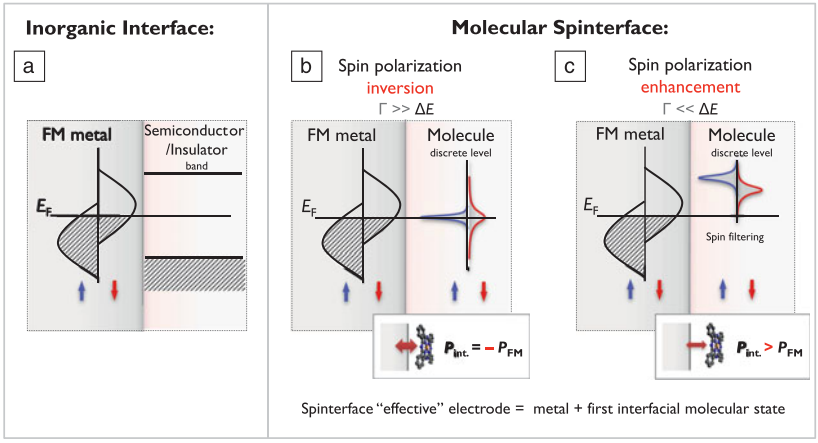

Figure 3. Illustration of the spinterface. (a) Usual representation of an inorganic interface with the conduction and valence band structure. (b–c) Representation of two examples of the molecular spinterface effect: inversion and enhancement (adapted from Reference 6). (b) Case of broadening being larger than the difference between molecular level energy and metal Fermi level ($\Gamma \gg \Delta E$). As the broadening area corresponds to only one spin state, a larger broadening ($\Gamma \propto D_{FM}^{\uparrow(\downarrow)}$) means a lower molecular density of states $D_{Int}^{\uparrow(\downarrow)}$. This induces an inversion of the spin polarization on the molecular orbital following Equation 3. (c) Opposite case where the energy difference between molecular level energy and metal Fermi level is larger than the broadening ($\Gamma \ll \Delta E$). The induced spin polarization can then be enhanced compared to the original spin polarization of the ferromagnet (FM) and can be compared to a spin-filter following Equation 4. Note: SC, semiconductor; E_F, Fermi energy level; P_{int}, spin polarization at the interface; P_{FM}, spin polarization of the FM electrode; $D_{FM}^{\uparrow(\downarrow)}$, DOS for spin up(down) of the FM metal; Γ, molecular energy level broadening.

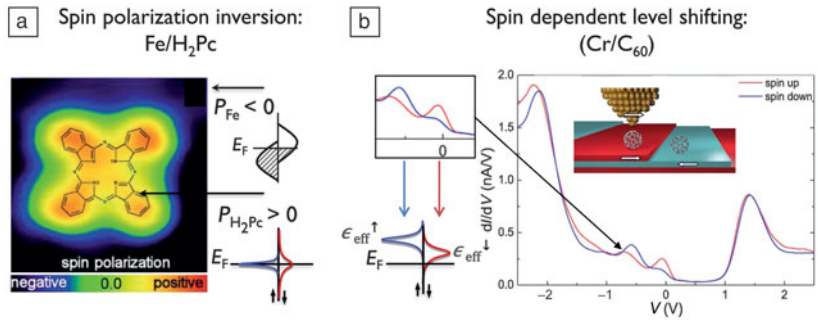

Figure 4. Experimental evidence of induced spin polarization inversion (a) and spin-dependent energy shifting on a single molecule (b). (a) Image of the spin polarization of a non-magnetic H_2Pc (Pc, phthalocyanines) molecule deposited on an iron surface by spin-polarized scanning tunneling microscopy experiments. While the iron surface spin polarization is negative (blue), the spin polarization on the molecule is positive (yellow-orange), highlighting the predicted spin polarization inversion on the H_2Pc orbitals (adapted from Reference 14). On the right side of the figure, the expected density of states of the Fe surface (black) and one of the molecules at the interface, when $\Gamma \gg \Delta E$, are schematically represented (adapted from Reference 6). (b) Spin-polarized scanning tunneling microscopy measurements on C_{60} molecules deposited on terraces with opposite magnetic configurations of a chromium surface (schematic representation in the inset). The difference in the conductance curves measured for the spin up (red) and spin down (blue) shows a spin-dependent energy shifting of the molecular levels up to 0.5 eV (adapted from Reference 18). The density of states expected for the molecule when $\Gamma \ll \Delta E$ is depicted on the left side of the image (adapted from Reference 6). Note: E_F, Fermi energy level; I, measured current; V, applied bias voltage; $\epsilon_{eff}^{\uparrow(\downarrow)}$, effective molecular level energy for spin up (down) when coupled to the surface.

Experimental evidence of spin-dependent hybridization

The spin-dependent hybridization at the FM metal/molecule interface has now been experimentally observed for several small molecules (mainly phthalocyanines (Pc), fullerene (C_{60}), and aluminum tris-hydroxyquinoline (Alq_3)) using surface-sensitive techniques as well as in spintronics devices. These experiments include spin-polarized scanning tunneling microscopy (SP-STM),[13–18] spin-polarized photoemission spectroscopy (SP-PES),[19,20] x-ray magnetic circular dichroism (XMCD),[20–22] spin-resolved two-photon photoemission spectroscopy,[23] and device magnetoresistance (MR) measurements.[6,24–26] For example, spin-dependent hybridized states have been observed for Alq_3 deposited on Fe surfaces by XMCD,[21] and for CuPc, FePc, CoPc,[19] and MnPc[20] on Co surfaces by SP-PES, wherein high spin polarization (80%) was measured at the Co/MnPc interface at room temperature. These results confirm the potential for spin hybridized states even at room temperature.

Spectroscopy measurements of spin-dependent hybridized molecular states

Examples highlighting the observation of spin polarization inversion and enhancement at the FM metal/molecule interface and spin-dependent shifting of the molecular level using different techniques are reviewed in this section.

Signatures of spin polarization inversion were observed[13,14,16] with SP-STM. For example, it was shown that spin polarization of the molecular orbitals of H_2Pc deposited on Fe was opposite to that of the Fe surface[14] (**Figure 4**a). This can be ascribed to the inversion case (Figure 3b) at the Fe/H_2Pc interface.

Spin polarization enhancement and spin-dependent energy shifting (ϵ) of molecular orbitals at the FM interface was directly measured for C_{60} molecules deposited on a chromium surface using SP-STM (Figure 4b). The resulting large spin-dependent energy shifting experienced by the molecular orbitals (up to 0.5 eV) induced a high tunneling magnetoresistance (TMR) ratio of up to 100% (not shown).[18] High MR of up to 60% was also observed for H_2Pc molecules deposited on cobalt islands and in contact with a STM cobalt tip.[17] The large MR in these systems was ascribed to spin-dependent broadening and shifting

of the molecular orbitals, leading to the spin polarization enhancement case depicted in Figure 3c.

More remarkably, it has been shown for CoPc that beyond the impact of adsorption geometry on the surface,[16] both inversion and enhancement of induced spin polarization can occur on different parts of the same molecule.[15] For example, an inversion of the spin polarization could be observed on carbon rings, whereas enhancement of spin polarization occurred on the cobalt center. This would be expected to occur if different parts of the molecule couple differently to the surface and can lead to engineering of molecular spintronics devices at the atomic scale.

Spin-dependent hybridized molecular states in spintronics devices

The effect of spin-dependent hybridized molecular states (spinterface) has not only been observed in STM experiments, it has also been evidenced in real solid-state spintronics devices, such as magnetic tunnel junctions. For example, a giant TMR effect (300%), which could be ascribed to the spin polarization enhancement case (see Figure 3c), was observed in $La_{0.7}Sr_{0.3}MnO_3/Alq_3/Co$ magnetic tunnel junctions (**Figure 5**a). The high TMR ratio observed corresponds to a spin polarization of at least $P = 60\%$ for the Alq_3/Co interface, showing a 30% enhancement compared to bare Co.[6]

The spin polarization inversion measured at the Co/CoPc interface by SP-STM[13,16] has also been observed in Co/CoPc/Co magnetic tunnel junctions (Figure 5b). The negative TMR observed in this system shows that the spin polarization is inverted at only one interface. Consequently, although there are two identical cobalt FM electrodes, the Co/CoPc and CoPc/Co (top interface) spinterfaces are drastically different.

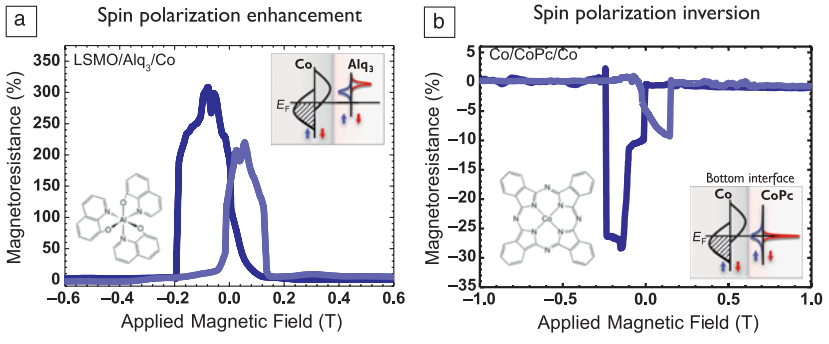

Figure 5. Tunneling magnetoresistance (TMR) experiments highlighting the enhancement and inversion of the spin polarization at the molecular level. Forward and backward magnetic field sweeps are, respectively, in light and dark blue. (a) High TMR in $La_{0.7}Sr_{0.3}MnO_3$ (LSMO)/Alq_3/Co magnetic tunnel junctions. The large TMR effect up to 300% is ascribed to an enhancement of at least 30% of the spin polarization at the Alq_3/Co interface. (b) Inverse TMR in Co/CoPc/Co magnetic tunnel junction. The inverse TMR means that the two interfacial spin polarizations have opposite sign. The inversion on the spin polarization occurs at the bottom Co/CoPc in agreement with spin-polarized scanning tunneling microscopy measurements performed on a single CoPc molecule on a cobalt surface.[13,16] Note: Alq_3, aluminum tris(8-hydroxyquinoline); Pc, phthalocyanines; E_F, Fermi energy level.

Lastly, it has been shown, using zinc methyl phenalenyl molecules deposited on a cobalt electrode, that the induced spin polarization can spread up to the second molecular layer with a lower coupling strength.[25] This was further supported by calculations (see the Atodiresei and Raman article in this issue). With hybridization being naturally weaker for the second molecular layer, the spin-dependent shifting of the molecular orbitals leads to an effective organic "spin polarizer" acting as a spin filter junction[6] (Figure 3c).

Conclusions and perspectives

Over the last few years, the fundamental role played by the FM metal/molecule interface in spintronics has been predicted and experimentally confirmed. It has been shown how, depending on the FM metal/molecule coupling strength, it would be possible to tune the interface spin polarization from enhancement to reversal of its sign. This has sparked a new field and has paved the way for new "spinterface" multifunctionalities where the functionality is governed by the interface. Overall, it could have an impact similar in vein to the symmetry filtering revolution in inorganic magnetic tunnel junctions, but relying on chemical engineering and leaving behind a perfect interface and a high crystallinity requirement. Spin-dependent hybridization can now be expected to be used in the tailoring of the resistive and magnetoresistive response of spintronics devices using functional molecules.

In these new crafted systems, a single multi-functional device could provide many spintronic functionalities. Indeed, spin-dependent broadening and shifting of the hybridized states could be tailored at will by molecular engineering and then tuned later on by external stimuli such as light, temperature, or a magnetic or electric field. Hence, for example, with molecules such as diazobenzenes, one could expect to switch the molecular conformation by the light or electric field controlling the coupling strength (weak/strong) and thus the spinterface response. Similarly, with redox molecules, one could electrically charge or discharge a carrier from the interface to the molecule, shifting the levels and modifying the coupling of the spinterface. Finally, with molecules such as spin crossover complexes, one could achieve the spinterface tailoring in multiple ways: optically, electrically, magnetically, or thermally. One can now envision spinterface as a way not only to tailor and enhance the spin injection into devices such as transistors or organic light-emitting diodes but also to design the (magneto-)resistive response, leading to multistate memories or memristive devices with a range of functionalities still waiting to be unveiled.

This uncharted field calls for intense interdisciplinary work, from modeling, transport, and surface spectroscopy measurements to

chemical design of new suitable molecules. Spinterfaces composed of self-assembled monolayers of functional molecules, where each part and function can be modulated independently (similar to a molecular LEGO building unit), appear to be more than highly promising candidates.

Acknowledgments

This work was partly funded through the European Union Seventh Framework Programme (FP7/2007–2013) under grant agreement No. 263104 and ANR agency (MELAMIN 2011-NANO-021). S.T. acknowledges the European Union FP7 CIG Marie Curie Actions under project SAMSFERE (FP7/2012–321739) and the Spanish MICINN for his JdC contract. P.S. wishes to thank the Institut Universitaire de France for a junior Fellowship. We also thank J. Arabski, E. Beaurepaire, I. Bergenti, S. Boukari, K. Bouzehouane, M. Bowen, S. Collin, C. Deranlot, E. Jacquet, and A. Riminucci for scientific discussions and assistance.

References

1. V. Dediu, M. Murgia, F.C. Matacotta, C. Taliani, S. Barbanera, *Solid State Commun.* **122**, 181 (2002).
2. Z.H. Xiong, D. Wu, Z. Valy Vardeny, J. Shi, *Nature* **427**, 821 (2004).
3. A.R. Rocha, V.M. García-Suárez, S.W. Bailey, C.J. Lambert, J. Ferrer, S. Sanvito, *Nat. Mater.* **4**, 335 (2005).
4. T.S. Santos, J.S. Lee, P. Migdal, I.C. Lekshmi, B. Satpati, J.S. Moodera, *Phys. Rev. Lett.* **98**, 016601 (2007).
5. V.A. Dediu, L.E. Hueso, I. Bergenti, C. Taliani, *Nat. Mater.* **8**, 707 (2009).
6. C. Barraud, P. Seneor, R. Mattana, S. Fusil, K. Bouzehouane, C. Deranlot, P. Graziosi, L. Hueso, I. Bergenti, V. Dediu, F. Petroff, A. Fert, *Nat. Phys.* **6**, 615 (2010).
7. S. Sanvito, *Nat. Phys.* **6**, 562 (2010).
8. S. Datta, *Quantum Transport: Atom to Transistor* (Cambridge University Press, New York, 2013).
9. H. Vázquez, R. Oszwaldowski, P. Pou, J. Ortega, R. Pérez, F. Flores, A. Kahn, *Europhys. Lett.* **65**, 802 (2007).
10. M.L. Perrin, C.J.O. Verzijl, C.A. Martin, A.J. Shaikh, R. Eelkema, J.H. van Esch, J.M. van Ruitenbeek, J.M. Thijssen, H.S.J. van der Zant, D. Dulić, *Nat. Nanotechnol.* **8**, 282 (2013).
11. J.S. Moodera, T.S. Santos, T. Nagahama, *J. Phys. Condens. Matter* **19**, 165202 (2007).
12. A.V. Ramos, M.J. Guittet, J.B. Moussy, R. Mattana, C. Deranlot, F. Petroff, C. Gatel, *Appl. Phys. Lett.* **91**, 122107 (2007).
13. C. Iacovita, M. Rastei, B. Heinrich, T. Brumme, J. Kortus, L. Limot, J. Bucher, *Phys. Rev. Lett.* **101**, 116602 (2008).
14. N. Atodiresei, J. Brede, P. Lazić, V. Caciuc, G. Hoffmann, R. Wiesendanger, S. Blügel, *Phys. Rev. Lett.* **105**, 066601 (2010).
15. J. Brede, N. Atodiresei, S. Kuck, P. Lazić, V. Caciuc, Y. Morikawa, G. Hoffmann, S. Blügel, R. Wiesendanger, *Phys. Rev. Lett.* **105**, 047204 (2010).
16. J. Brede, R. Wiesendanger, *Phys. Rev. B: Condens. Matter* **86**, 184423 (2012).
17. S. Schmaus, A. Bagrets, Y. Nahas, T.K. Yamada, A. Bork, M. Bowen, E. Beaurepaire, F. Evers, W. Wulfhekel, *Nat. Nanotechnol.* **6**, 185 (2011).
18. S.L. Kawahara, J. Lagoute, V. Repain, C. Chacon, Y. Girard, S. Rousset, A. Smogunov, C. Barreteau, *Nano Lett.* **12**, 4558 (2012).
19. S. Lach, A. Altenhof, K. Tarafder, F. Schmitt, M.E. Ali, M. Vogel, J. Sauther, P.M. Oppeneer, C. Ziegler, *Adv. Funct. Mater.* **22**, 989 (2012).
20. F. Djeghloul, F. Ibrahim, M. Cantoni, M. Bowen, L. Joly, S. Boukari, P. Ohresser, F. Bertran, P. Lefèvre, P. Thakur, F. Scheurer, T. Miyamachi, R. Mattana, P. Seneor, A. Jaafar, C. Rinaldi, S. Javaid, J. Arabski, J.P. Kappler, W. Wulfhekel, N.B. Brookes, R. Bertacco, A. Taleb-Ibrahimi, M. Alouani, E. Beaurepaire, W. Weber, *Sci. Rep.* **3**, 1272 (2013).
21. Y. Zhan, E. Holmstrom, R. Lizarraga, O. Eriksson, X. Liu, F. Li, E. Carlegrim, S. Stafstrom, M. Fahlman, *Adv. Mater.* **22**, 1626 (2010).
22. T.L.A. Tran, P.K.J. Wong, M.P. De Jong, W.G. van der Wiel, Y.Q. Zhan, M. Fahlman, *Appl. Phys. Lett.* **98**, 222505 (2011).
23. S. Steil, N. Großmann, M. Laux, A. Ruffing, D. Steil, M. Wiesenmayer, S. Mathias, O.L.A. Monti, M. Cinchetti, M. Aeschlimann, *Nat. Phys.* **9**, 242 (2013).
24. L. Schulz, L. Nuccio, M. Willis, P. Desai, P. Shakya, T. Kreouzis, V.K. Malik, C. Bernhard, F.L. Pratt, N.A. Morley, A. Suter, G.J. Nieuwenhuys, T. Prokscha, E. Morenzoni, W.P. Gillin, A.J. Drew, *Nat. Mater.* **10**, 39 (2011).
25. K.V. Raman, A.M. Kamerbeek, A. Mukherjee, N. Atodiresei, T.K. Sen, P. Lazić, V. Caciuc, R. Michel, D. Stalke, S.K. Mandal, S. Blügel, M. Münzenberg, J.S. Moodera, *Nature* **493**, 509 (2013).
26. K. Yoshida, I. Hamada, S. Sakata, A. Umeno, M. Tsukada, K. Hirakawa, *Nano Lett.* **13**, 481 (2013). □